

Effect of heat treatment on microstructures and mechanical properties of high vacuum die casting Mg–8Gd–3Y–0.4Zr magnesium alloy

Zhi-qin WANG¹, Bin ZHANG¹, De-jiang LI¹, Robert FRITZSCH²,
Xiao-qin ZENG^{1,3}, Hans J. ROVEN^{2,4}, Wen-jiang DING^{1,3}

1. National Engineering Research Center of Light Alloy Net Forming, School of Materials Science and Engineering, Shanghai Jiao Tong University, Shanghai 200240, China;
2. Department of Materials Science and Engineering, Norwegian University of Science and Technology, Trondheim 7491, Norway;
3. Key State Laboratory of Metal Matrix Composite, Shanghai Jiao Tong University, Shanghai 200240, China;
4. Center for Advanced Materials, Qatar University, Doha POB 2713, Qatar

Received 17 October 2013; accepted 17 November 2014

Abstract: The microstructure, the content of compounds, mechanical properties and fracture behavior of high vacuum die casting Mg–8Gd–3Y–0.4Zr alloy (mass fraction, %) under T4 condition and T6 condition were investigated. The microstructure for the as-cast Mg–8Gd–3Y–0.4Zr alloy mainly consists of α -Mg and eutectic Mg₂₄(Gd,Y)₅ compound. After solution treatment, the eutectic compounds dissolve massively into the Mg matrix. The main composition of solution-treated alloys is supersaturated α -Mg and cuboid-shaped phase. The T4 heat treated samples have increasing cuboidal particles with the increase of heat treatment temperature, which turn out good mechanical properties. The optimum T4 heat treatment for high vacuum die cast Mg–8Gd–3Y–0.4Zr alloy is 475 °C, 2 h according to microstructure results. The optimum ultimate strength and elongation of solution-treated Mg–8Gd–3Y–0.4Zr alloy are 222.1 MPa and 15.4%, respectively. The tensile fracture mode of the as-cast, and T6 heat treated alloys is transgranular quasi-cleavage fracture.

Key words: Mg–8Gd–3Y–0.4Zr alloy; heat treatment; microstructure; mechanical property; fracture behavior

1 Introduction

Magnesium and its alloys are the lightest structural alloys developed so far and have great potential for lightweight applications, ranging from portable electronic devices to automobile parts. High pressure die-casting (HPDC) is a dominant processing route to produce magnesium components due to its excellent productivity for the manufacture of complex, thin-walled, and near net shape parts [1].

During the die-casting process, the injection stroke can cause a jet of molten metal to hit the far end of the mold cavity and then splash backward. This produces highly turbulent conditions, and introduces a large amount of air, which mixes the lubricants and volatile fumes into the casting. This kind of entrapped gas in the

alloy melt will not only lead to decreased mechanical properties, but also bring about gas porosity in the casting, which will blister upon solution heat treatments at high temperatures. It is well known that evacuation of the die cavity is an effective method to produce high-quality castings free of defects associated with cavity gases. Super vacuum die-casting (SVDC), as a special variant of the HPDC process using a vacuum level of below 6 kPa, has been developed to produce high-integrity parts with improved monotonic mechanical properties as reported for AZ91 alloy [2,3]. Further studies [4–6] also showed improved fatigue strength and corrosion resistance of SVDC castings compared with conventional HPDC samples.

It has been demonstrated that rare earth metals (RE) are the most effective elements to improve the strength of magnesium especially [7]. Among different kinds of

Foundation item: Projects (51171113, 51301107) supported by the National Natural Science Foundation of China; Projects (2012M511089, 2013T60444) supported by the China Postdoctoral Science Foundation; Projects (2011BAE22B02, 2011DFA50907) supported by the Ministry of Science and Technology of China

Corresponding author: De-jiang LI; Tel: +86-21-34203730; E-mail: lidejiang@sjtu.edu.cn
DOI: 10.1016/S1003-6326(14)63530-5

Mg–RE alloys [8–12], Mg–Gd–Y system is one of the most promising candidates due to its rapid age-hardening response and very good thermal stability of the main strengthening phase up to 250 °C. Many investigations related to the microstructure and mechanical properties of the Mg–Gd–Y system have been reported [13–15]. According to XU's research results [16], the Mg–Gd–Y alloy with the ratio of $x(\text{Gd})/x(\text{Y}) \approx 8/3$ shows excellent mechanical properties, as it is cast or heat treated. Therefore, Mg–8Gd–3Y–0.1Zr alloy is a research focus in this work.

However, few systematical research reports on heat treatment process of Mg–8Gd–3Y–0.4Zr alloy obtained by SVDC with respect to microstructures, mechanical properties and fracture behavior analysis were found. The present work aims at optimizing heat treatment process of super vacuum die-cast Mg–8Gd–3Y–0.4Zr (named as GW83K) and investigating its corresponding microstructure, mechanical properties at room temperature and fracture behavior with various analysis methods.

2 Experimental

GW83K (Mg–7.97Gd–2.56Y–0.29Zr, mass fraction, %) alloy was used in the SVDC experiments (TOYO, BC-350V5), and the alloy was melted and injected into the mold at 983 K (710 °C) with the temperature of the mold at 473 K (200 °C). The vacuum level of the casting process was kept at about 6 kPa using the VDS vacuum system.

Referred to HE [17] and XU's [16] former research results and Mg–Gd–Y ternary phase diagram, the solution heat treatment conditions were determined to be 723, 748, 773 K (450, 475, 500 °C) for 2, 4, 6 h separately followed by water quenching and then part of the solution-treated samples were aged at 498 K (225 °C) in oil bath.

The microstructures of as-cast and heat-treated samples were observed using optical microscope (OM, Zeiss, Axio Observer A1), scanning electron microscopes (SEM, JEOL, JSM-7600F and Hitachi, SU-6600). The OM and SEM samples were mechanically polished and then etched in a picric acid 2,4,6-trinitrophenol solution. The quantitative analysis of the chemical compositions of the phases in the microstructure was performed using energy dispersive X-ray spectrometer (EDS) equipped on the SEM. Phase compositions were scanned by X-ray diffraction. Tensile properties tests of the alloys were performed at the initial strain rate of $5 \times 10^{-4} \text{ s}^{-1}$ referred to GB/T2008—2002 using cylindrical specimen with marked dimension of 15 mm in gauge length, 2 mm in thickness and 3.5 mm in width on Zwick/Roell Z020

tensile machine at room temperature. The fracture surface and profiles were analyzed by SEM as well.

3 Results and discussion

3.1 Microstructure of as-cast alloy

The microstructure of the as-cast GW83K alloy by OM analysis is shown in Fig. 1(a). The microstructure of the as-cast GW83K alloy consists of coarse α -Mg dendrites and network eutectic compounds. The eutectic compounds mainly distribute at grain boundaries. The grain size of the alloy is not uniform with some of them under 10 μm and some of them over 20 μm .

Figures 1(b)–(d) show the secondary electron SEM images and EDS element point results of the as-cast sample. It can be seen that Gd and Y elements are mainly concentrated on the compounds which are along the grain boundaries. However, the Mg element is not rich in this area. The EDS of point A shows that the contents of Gd and Y elements which are concentrated on the grain boundaries are 20.0% and 3.63% (mass fraction), respectively. This results are about two times those of point B.

Figure 2 shows the corresponding XRD pattern of the as-cast GW83K alloy. According to the XRD results, the alloy contains two different phases: α -Mg phase and the eutectic phase consisting of $\text{Mg}_{24}(\text{Gd},\text{Y})_5$. Corresponding to the SEM and EDS results, it can be identified that the eutectic compounds which are concentrated along the grain boundaries consist of $\text{Mg}_{24}(\text{Gd},\text{Y})_5$. This result is consistent with HE's research [17], which shows that the $\text{Mg}_{24}(\text{Gd},\text{Y})_5$ phase is a body-centered cubic structure and $a=11.2 \text{ \AA}$.

3.2 Microstructure of solution-treated alloys

Figure 3(a) shows an optical micrograph of the solution treated alloy at 773 K (500 °C) for 6 h, from which it can be seen that almost all the eutectic compounds in the as-cast sample have been dissolved into the matrix after solution treatment. Gd and Y atoms dissolve into the magnesium matrix and form supersaturated solid solution. Moreover, some unevenly distributed small granular black dots are observed along grain boundaries and inside the grains. Figure 3(b) shows the magnified SEM image of these black dots in a solution treated (500 °C, 6 h) GW83K alloy. It can be seen that these dots have cuboid shape.

Figure 4 presents EDS point results of the cuboid-shaped phases in the alloys solution treated at 723 K (450 °C), 748 K (475 °C) and 773 K (500 °C) for 6 h, respectively. It can be seen that the cuboid-shaped dots are rich in Gd and Y elements while lack of Mg element. This is consistent with HE's results [17], which identifies

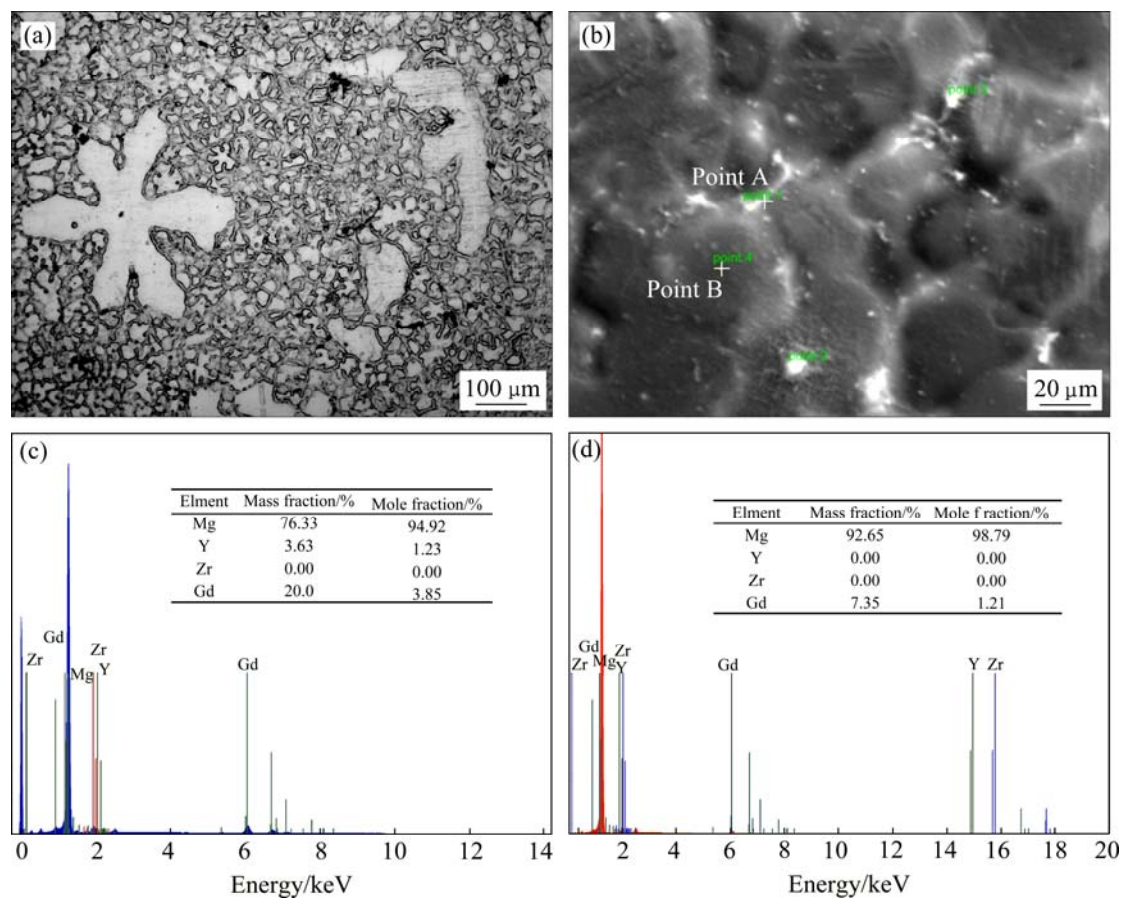


Fig. 1 Optical (a) and SEM (b) images of as-cast GW83K alloy, and EDS results of point A (c) and point B (d)

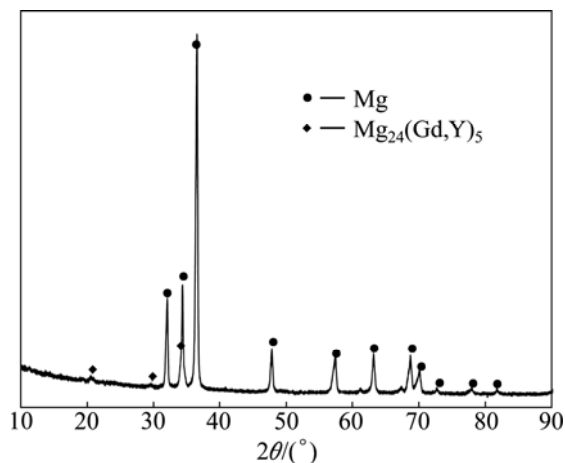


Fig. 2 XRD pattern of as-cast GW83K alloy

that the cuboid-shaped phases have face-centered cubic structure and lattice constant is 5.6 Å. The mass fractions of Gd element in the alloys solution treated at 723 K (450 °C) and 748 K (475 °C) are lower than those observed in the alloy solution treated at 773 K (500 °C) for 6 h. The high solution temperature brings increasing growth of cuboid-shaped phase. Figure 5 shows the cuboid-shaped phases in the SEM image marked by Image Pro software in red color. Table 1 shows the

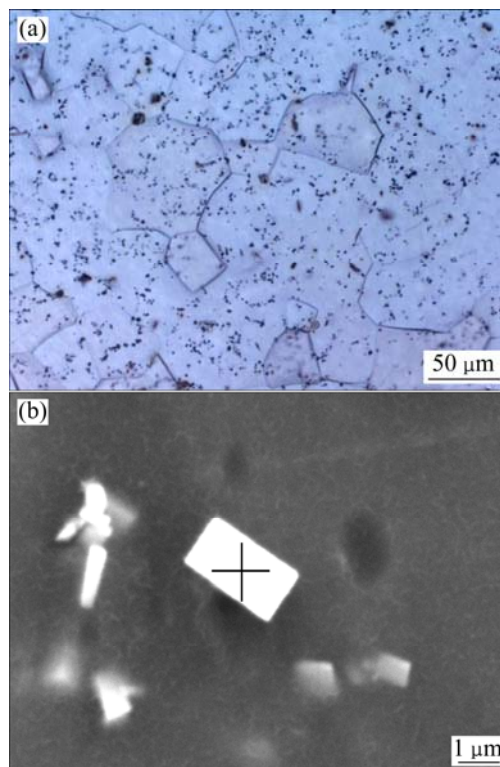


Fig. 3 Microstructure (a) and SEM image of black dots (b) in solution-treated (500 °C, 6 h) GW83 alloy

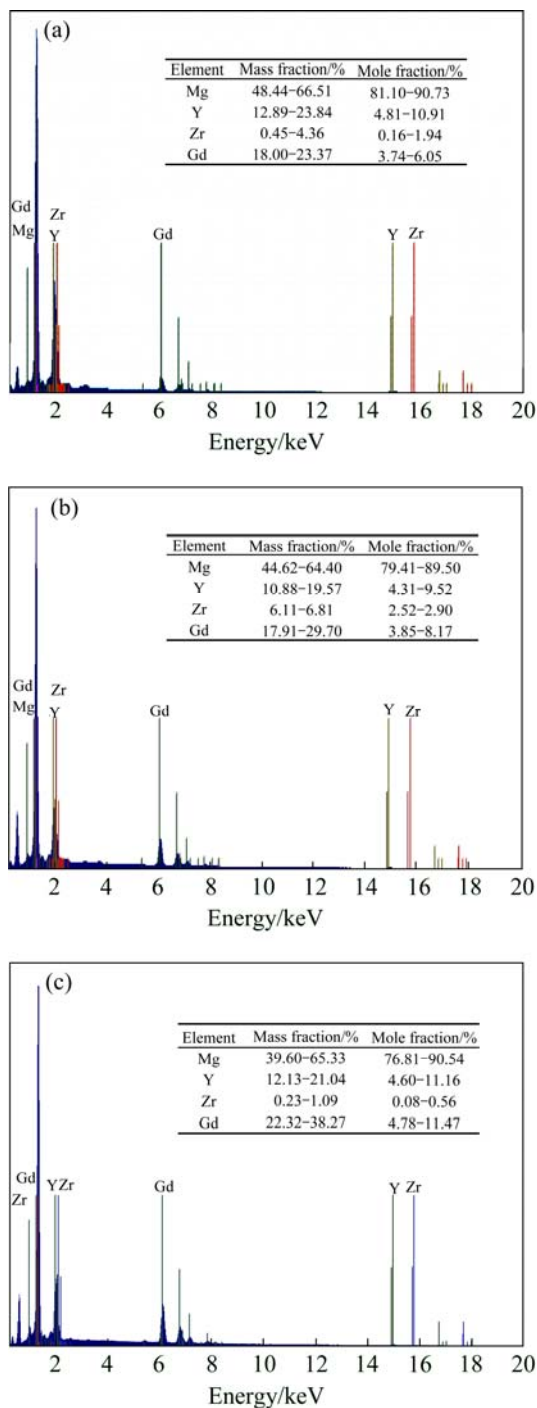


Fig. 4 EDS point results of cuboid phases in different solution treated GW83 alloys: (a) 450 °C, 6 h; (b) 475 °C, 6 h; (c) 500 °C, 6 h

quantity and area of the cuboid-shaped phases in the solution-treated alloy detected by Image Pro software. It presents that the area of cuboid-shaped phases increases with the increase of the solution temperature. This identifies that solution temperature has an effect on the growth of cuboid phases.

Figure 6 shows the optical micrographs of the solution treated alloys with various temperatures and

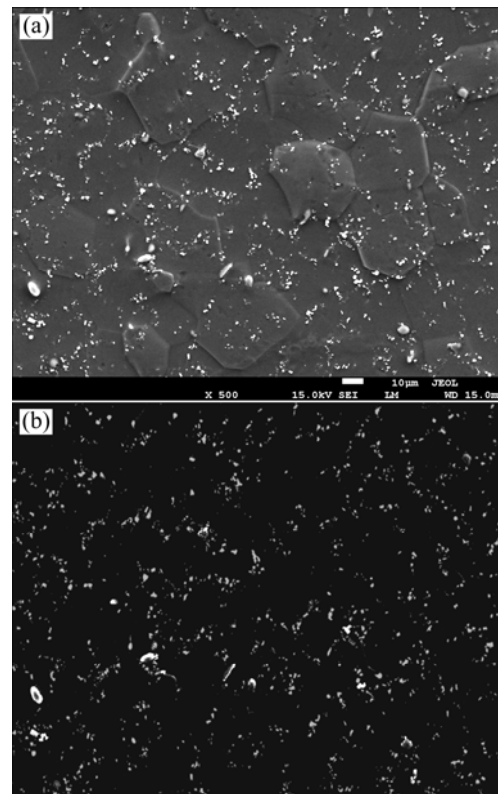


Fig. 5 SEM image of GW83 alloy solution-treated at 773 K (500 °C) for 6 h (a) and corresponding Image Pro detected result (b)

Table 1 Quantity and area of cuboid-shaped phases in different solution-treated GW83 alloys

Solution-treated condition	Quantity of cuboid-shaped phases	Area of cuboid-shaped phases/cm ²	Average area of cuboid-shaped phase/mm ²
723 K, 6 h	2265	247.62	10.93
748 K, 6 h	2574	325.27	12.64
773 K, 6 h	1796	318.66	17.74

holding time. It can be seen that samples solution treated at the same temperature tend to have increasing grain sizes with increasing the holding time. Samples solution treated at 723 K (450 °C) obtain inhomogeneous grain sizes. Some grains are able to grow and some of them are still small. This is due to the low solution temperature which is not able to give enough activation energy for entire grain growth. According to the desired outcome of having a microstructure with a small grain size and few remnant second phases, an optimal solution condition could be selected. An average grain size of (29.38±2) μm in the alloy could be achieved after being solution treated at 748 K (475 °C) for 2 h. This is the optimal solution condition because the grain size maintains small, and most of the grains are homogeneous with few remaining eutectic compounds.

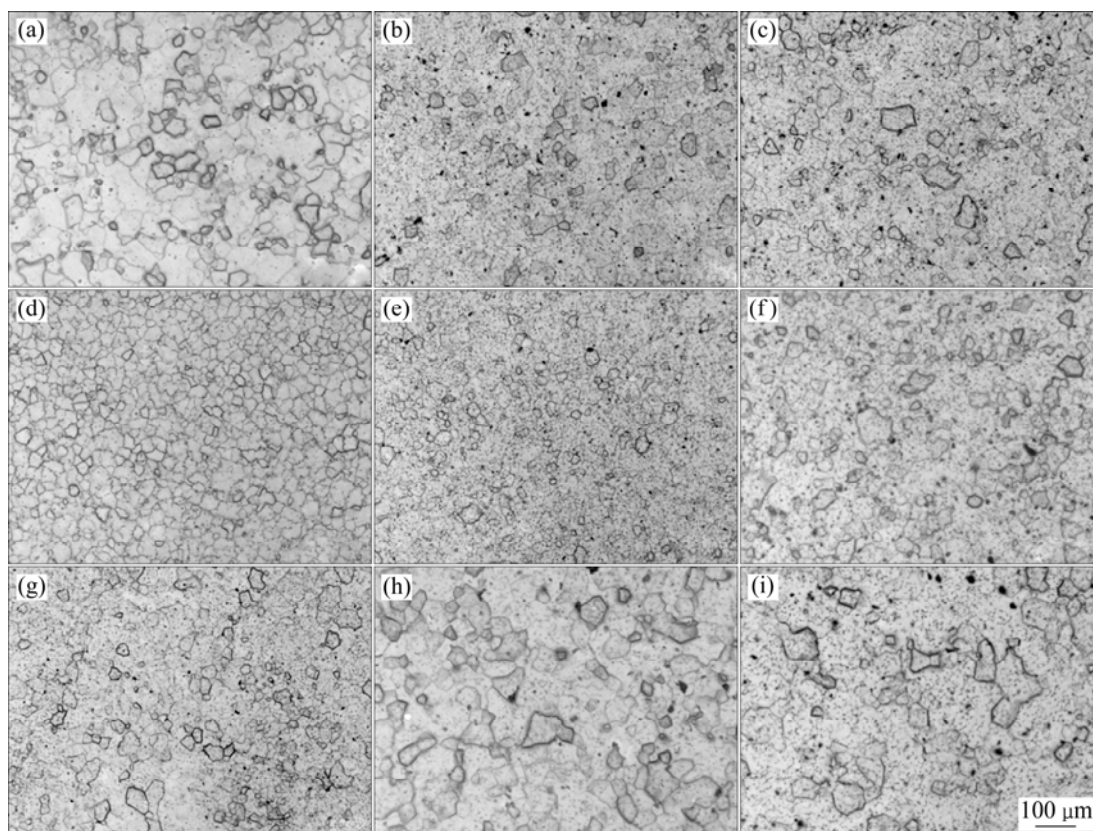


Fig. 6 Optical micrographs of solution-treated samples with different temperatures and holding time: (a) 723 K, 2 h; (b) 723 K, 4 h; (c) 723 K, 6 h; (d) 748 K, 2 h; (e) 748 K, 4 h; (f) 748 K, 6 h; (g) 773 K, 2 h; (h) 773 K, 4 h; (i) 773 K, 6 h

3.3 Mechanical properties

Table 2 gives the tensile properties of the as-cast alloy and solution treated alloys under different solution conditions. It can be seen that the elongation of the solution-treated alloy increases but the yield strength (YS) and ultimate tensile strength (UTS) decrease compared with those of the as-cast alloy. This can be explained that the eutectic compounds presented in the as-cast alloy are mostly dissolved into the matrix during the solution

Table 2 Tensile properties of as-cast GW83 and solution-treated alloys at different temperatures and holding time

Heat treatment condition	Yield strength/MPa	Ultimate tensile strength/MPa	Elongation/%
As cast	194.8	236.8	7.3
723 K, 2 h	165.7	208.5	9.0
723 K, 4 h	147.6	216.0	14.0
723 K, 6 h	160.0	216.3	11.6
748 K, 2 h	144.3	210.0	10.8
748 K, 4 h	154.8	216.6	13.1
748 K, 6 h	149.0	214.4	12.0
773 K, 2 h	150.0	213.2	11.7
773 K, 4 h	152.4	224.4	15.8
773 K, 6 h	155.8	222.1	15.4

treatment, which reduces barriers to dislocation slip. It can be observed that the elongation and UTS values have an increasing trend for those samples solution treated at high temperature but with the same holding time. Samples solution treated at 773 K (500 °C) for 6 h obtain high elongation of 15.4% and high UTS of about 222.1 MPa. This is due to the increasing dissolution of eutectic compounds with increasing solution temperature, which breaks the matrix phase and changes the brittleness of the alloy.

Table 3 gives tensile properties of all the solution treated GW83 alloys after aging treatment at 498 K (225 °C) for 16 h. It can be observed that yield strengths of alloys is improved by 22.5–90.9 MPa after T6 treatment. The maximum yield strength of T6-treated alloys is 240.9 MPa and that of T4-treated alloys is 165.7 MPa. The improvement of yield strength is related to the precipitation process of T6 treatment, which is $\alpha \rightarrow \beta'' \rightarrow \beta$ (Mg5Gd: FCC) [16]. The precipitation of β'' phase in peak-aging process is the main reason for improving the yield strength.

3.4 Fractography

Figure 7 shows the fracture surfaces of the tensile specimens of the GW83K alloy in different conditions. It

Table 3 Tensile properties of all solution-treated GW83K alloys after peak-aging treatment at 498 K (225 °C)

Solution-treated condition	Yield strength/MPa	Ultimate tensile strength/MPa	Elongation/%
723 K, 2 h	217.6	269	8.0
723 K, 4 h	237.2	251.8	2.1
723 K, 6 h	209.9	215.7	1.5
748 K, 2 h	217.2	241.9	3.4
748 K, 4 h	210.3	261.8	10.8
748 K, 6 h	209.5	246.3	5.4
773 K, 2 h	240.9	274.8	7.2
773 K, 4 h	174.9	226.9	7.7
773 K, 6 h	192.2	233	4.4

is observed that there are some cleavage planes, evident tearing ridges and a few dimples in the fracture surfaces of as-cast alloy. Comparatively, there are mainly cleavage planes and tearing ridges observed in the fracture surfaces of solution-treated alloy. The eutectic compounds have been dissolved after solution treatment, the cleavage planes become wide and river patterns with small steps are well developed. Figure 7(c) shows the fracture surfaces of the tensile specimens of the GW83K alloy T6-treated at 498 K (225 °C) for 16 h. It can be seen that there are increasing secondary cracks which are close to the main cracks (the secondary cracks are marked by white arrows in the images). This indicates that the fracture mode of solution-treated alloy is transgranular cleavage fracture while the fracture mode of as-cast alloy and T6-peak-aging alloy is transgranular quasi-cleavage fracture.

4 Conclusions

1) The microstructures for the SVDC-cast Mg–8Gd–3Y–0.4Zr alloy mainly consist of α -Mg and eutectic $Mg_{24}(Gd,Y)_5$ compound. After solution treatment, the eutectic compounds dissolve massively into the Mg matrix. The main composition of solution treated alloys is supersaturated α -Mg and cuboid-shaped phase.

2) The ductility of the solution treated alloy is improved significantly compared with that of the as-cast alloy. Samples solution treated at 773 K (500 °C) for 6 h obtain comparatively high elongation of about 15.4% and UTS of about 222.1 MPa. This is due to the increasing production of small cuboid-shaped phase in the alloy.

3) Taking grain growth and remnant second phases into consideration, an average grain size of $(29.38 \pm 2) \mu m$ in the alloy could be achieved after being solution treated at the optimum condition of 748 K (475 °C) and 2 h. Compared with the T4 samples, the YS of the T6 sample increases, which is influenced by the precipitation of β'' phase.

4) The fracture mode of solution treated alloy is transgranular cleavage fracture while the fracture mode of as-cast alloy and T6-peak-aging is transgranular quasi-cleavage fracture.

References

- [1] TERADA Y, DAIGO I, SATO T. Dislocation analysis of die-cast Mg–Al–Ca alloy after creep deformation [J]. *Material Science Engineering A*, 2009, 523(1–2): 214–19.
- [2] BROWN Z, LUO A A, MUSSER M, OUIMET L J, SADAYAPPAN K, ZINDEK J, BEALS R. Development of super vacuum die casting process for magnesium alloys [J]. *North American Die Casting*

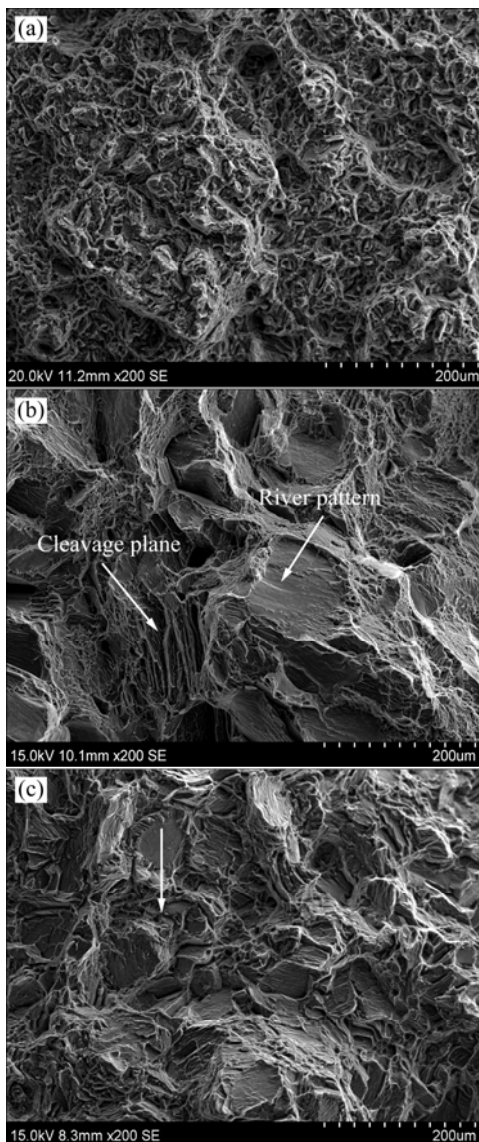


Fig. 7 Typical SEM images showing fracture surfaces of tensile samples: (a) As-cast; (b) Solution-treated at 773 K (500 °C) for 6 h; (c) T6-treated at 498 K (225 °C) for 16 h

- Association Transactions, Wheeling, 2009, T09-043: 723–729.
- [3] SADAYAPPANK, KASPRZAK W, BROWN Z, OUMET L, LUO A A. Characterization of magnesium automotive components produced by super-vacuum die casting process [J]. Materials Science Forum, 2009, 618–619: 381–386.
- [4] KRAUM SCHOLTES B. Thermal fatigue of magnesium-base alloy AZ91 [J]. Material Science and Engineering Technology, 2008, 39(8): 562–570.
- [5] PATEL H A, RASHIDI N, CHEN D L, BHOLE S D, LUO A A. Cyclic deformation behavior of a super-vacuum die cast magnesium alloy [J]. Material Science Engineering A, 2012, 546(1): 72–81.
- [6] WEN Wei, LUO A A, ZHAI Tong-guang, JIN Yan, CHENG Y, HOFFMANN I. Improved bending fatigue and corrosion properties of a Mg–Al–Mn alloy by super vacuum die casting [J]. Scripta Materialia, 2012, 67(11): 879–82.
- [7] LIU Wen-cai, DONG Jie, SONG Xu, BELNOUE J P, HOFMANN F, DING Wen-jiang, KORSUNSKY A M. Effect of microstructures and texture development on tensile properties of Mg–10Gd–3Y alloy [J]. Materials Science and Engineering A, 2011, 528(6): 2250–2258.
- [8] GAO Xiang, HE Shang-ming, ZENG Xiao-qin, PENG Li-ming, DING Wen-jiang, NIE Jian-feng. Microstructure evolution in a Mg–15Gd–0.5Zr (wt.%) alloy during isothermal aging at 250 °C [J]. Material Science and Engineering A, 2006, 431(1–2): 322–327.
- [9] NIE Jian-feng, GAO Xiang, ZHU Su-ming. Enhanced age hardening response and creep resistance of Mg–Gd alloys containing Zn [J]. Scripta Materialia, 2005, 53(9): 1049–1053.
- [10] GAO Xiang, NIE Jian-feng. Enhanced precipitation-hardening in Mg–Gd alloys containing Ag and Zn [J]. Scripta Materialia, 2008, 58(8): 619–622.
- [11] ZHENG Kai-yun, DONG Jie, ZENG Xiao-qin, DING Wen-jiang. Precipitation and its effect on the mechanical properties of a cast Mg–Gd–Nd–Zr alloy [J]. Material Science and Engineering A, 2008, 489(1–2): 44–54.
- [12] LIANG Shu-quan, GUAN Di-kai, CHEN Liang, GAO Zhao-he, TANG Hui-xiang, TONG Xu-ting, XIAO Rui. Precipitation and its effect on age-hardening behavior of sand-cast Mg–Gd–Y alloy [J]. Materials and Design, 2011, 32(1): 361–364.
- [13] LIU Wen-cai, DONG Jie, ZHANG Ping, KORSUNSKY A M, SONG Xu, DING Wen-jiang. Improvement of fatigue properties by shot peening for Mg–10Gd–3Y alloy under different conditions [J]. Materials Science and Engineering A, 2011, 528(18): 5935–5944.
- [14] DONG Jie, LIU Wen-cai, SONG Xu, ZHANG Ping, DING Wen-jiang, KORSUNSKY A M. Influence of heat treatment on fatigue behavior of high-strength Mg–10Gd–3Y alloy [J]. Materials Science and Engineering A, 2010, 527(21–22): 6053–6063.
- [15] LIU Wen-cai, WU Guo-hua, ZHAI Chun-quan, DING Wen-jiang, KORSUNSKY A M. Grain refinement and fatigue strengthening mechanisms in as-extruded Mg–6Zn–0.5Zr and Mg–10Gd–3Y–0.5Zr magnesium alloys by shot peening [J]. International Journal of Plasticity, 2013, 49: 16–35.
- [16] XU Xing-hong. Study on heat treatment process of GW83 alloy [D]. ShengYang: Liaoning Technical University, 2005. (in Chinese)
- [17] HE Shang-ming. Study on the microstructural evolution, properties and fracture behavior of Mg–Gd–Y–Zr (–Ca) alloys [D]. Shanghai: Shanghai Jiao Tong University, 2007. (in Chinese)

热处理工艺对高真空压铸 Mg–8Gd–3Y–0.4Zr 镁合金组织及力学性能的影响

王梳沁¹, 张彬¹, 李德江¹, Robert FRITZSCH², 曾小勤^{1,3}, Hans J. ROVEN^{2,4}, 丁文江^{1,3}

1. 上海交通大学 材料科学与工程学院, 轻合金精密成型国家工程研究中心, 上海 200240;
2. Department of Materials Science and Engineering, Norwegian University of Science and Technology, Trondheim 7491, Norway;
3. 上海交通大学 金属基复合材料国家重点实验室, 上海 200240;
4. Center for Advanced Materials, Qatar University, Doha POB 2713, Qatar

摘要: 研究 T4 和 T6 热处理状态下高真空压铸 Mg–8Gd–3Y–0.4Zr(质量分数, %)合金的微观组织、化合物含量、力学性能及断裂行为。铸态 Mg–8Gd–3Y–0.4Zr 合金微观组织主要由 α -Mg 和共晶 Mg₂₄(Gd,Y)₅ 化合物组成。经固溶处理后, 共晶化合物大量溶解于镁基体, 合金主要含过饱和 α -Mg 及方块相。固溶合金中方块相的含量随固溶温度的升高而增大, 力学性能也有所提高。根据微观组织结果, 确定 475 °C, 2 h 为 Mg–8Gd–3Y–0.4Zr 合金最优固溶方案。合金的最佳屈服强度为 222.1 MPa, 延伸率可达 15.4%。铸态, T4 状态下和 T6 状态下合金的拉伸断裂模式为穿晶准解理断裂。

关键词: Mg–8Gd–3Y–0.4Zr 合金; 热处理工艺; 微观组织; 力学性能; 断裂行为

(Edited by Yun-bin HE)